

Article

Photocatalytic Coproduction of Deoxybenzoin and H₂ through Tandem Redox Reactions

Nengchao Luo, Tingting Hou, Shiyang Liu, Bin Zeng, Jianmin Lu, Jian Zhang, Hongji Li, and Feng Wang

ACS Catal., Just Accepted Manuscript • DOI: 10.1021/acscatal.9b03651 • Publication Date (Web): 04 Dec 2019

Downloaded from pubs.acs.org on December 12, 2019

Just Accepted

"Just Accepted" manuscripts have been peer-reviewed and accepted for publication. They are posted online prior to technical editing, formatting for publication and author proofing. The American Chemical Society provides "Just Accepted" as a service to the research community to expedite the dissemination of scientific material as soon as possible after acceptance. "Just Accepted" manuscripts appear in full in PDF format accompanied by an HTML abstract. "Just Accepted" manuscripts have been fully peer reviewed, but should not be considered the official version of record. They are citable by the Digital Object Identifier (DOI®). "Just Accepted" is an optional service offered to authors. Therefore, the "Just Accepted" Web site may not include all articles that will be published in the journal. After a manuscript is technically edited and formatted, it will be removed from the "Just Accepted" Web site and published as an ASAP article. Note that technical editing may introduce minor changes to the manuscript text and/or graphics which could affect content, and all legal disclaimers and ethical guidelines that apply to the journal pertain. ACS cannot be held responsible for errors or consequences arising from the use of information contained in these "Just Accepted" manuscripts.

Photocatalytic Coproduction of Deoxybenzoin and H₂ through Tandem Redox Reactions

Nengchao Luo,^{1,2} Tingting Hou,³ Shiyang Liu,^{1,2} Bin Zeng,^{1,2} Jianmin Lu,¹ Jian Zhang,¹ Hongji Li,^{1,2}

Feng Wang^{1*}

¹ State Key Laboratory of Catalysis, Dalian National Laboratory for Clean Energy, Dalian Institute of Chemical Physics, Chinese Academy of Sciences, Dalian 116023, P. R. China

² University of Chinese Academy of Sciences, Beijing 100049, P. R. China

³ School of Materials Science and Engineering, Central South University, Changsha 410083, P. R. China

Corresponding author:

*Feng Wang, wangfeng@dicp.ac.cn

ABSTRACT

Photocatalytic H₂ evolution from organic feedstocks with simultaneous utilization of photogenerated holes achieves solar energy storage and coproduces value-added chemicals. Here we show visible light H₂ production from benzyl alcohol (BAL) with controllable generation of deoxybenzoin (DOB) or benzoin (BZ) through tandem redox reactions. Particularly, DOB synthesis circumvents the use of expensive feedstocks and environmentally unfriendly catalysts that are required previously. Under the irradiation of blue LEDs, the key of steering the major product to DOB rather than BZ is to decrease the conduction band bottom potentials of the ZnIn sulfide catalysts by increasing the Zn/In ratio, which results in the dehydration of intermediate hydrobenzoin (HB) to DOB proceeding in a redox-neutral mechanism and consuming an electron-hole pair. As a proof of concept, this method is used to synthesize DOB derivatives in gram scale.

Key words: Photocatalysis; dehydrogenation; dehydration; C–C coupling; deoxybenzoin; ZnIn₂S₄

INTRODUCTION

Photocatalytic transformation of organic feedstocks has emerged as a sustainable and environmentally benign method to produce value-added products.¹⁻³ By virtue of light irradiation, oxidative holes and reductive electrons are generated in semiconductors, which results in oxidation and reduction of organic moieties, respectively, and affords targeted products. Due to the formation of charges (i.e. holes and electrons) that are in excited states, photocatalysis is able to achieve uphill reactions that are usually possible at elevated temperatures for thermocatalysis.⁴⁻⁵ Therefore, if H₂ is coproduced in photocatalytic selective transformation of organic feedstocks, the whole reaction will maximize the merit of photocatalysis. In this context, use of solar light to construct C–C bond with H₂ production receives much attention due to the straightforward production of value-added products from readily available feedstocks without the use of hazardous catalysts and additives.⁶⁻⁷ Previous works have achieved direct synthesis of ethylene glycol from methanol,⁸ ethane or benzene from methane,⁹⁻¹⁰ together with H₂ production.¹¹ These state-of-the-art processes demonstrate the tremendous potential of photocatalysis in producing H₂ with simultaneous utilization of small molecules as building blocks to provide value-added products through C–H bond dehydrocoupling.

Production of deoxybenzoin (DOB) from benzyl alcohol (BAL) is such an example. DOB was industrially prepared from phenylacetic acid and benzene by AlCl₃ catalyzed C–C bond coupling. The process requires functionalization of phenylacetic acid to phenylacetyl chloride by stoichiometric PCl₃ or SOCl₂ prior to the C–C bond coupling.¹²⁻¹³ Other reported methods required the pre-functionalization of starting molecules or use expensive substrates alternatively (Scheme. S1).¹⁴⁻¹⁶ Thus, it is desirable to develop processes for DOB production using readily available and environmentally benign feedstocks. Moreover, if H₂ is also produced in the conversion of BAL to

1
2
3
4 DOB, the whole process will achieve the coproduction of a clean energy vector and a very high value-
5
6 added product.¹⁷⁻¹⁹
7

8
9 One way to produce DOB from BAL is by tandem dehydrocoupling and dehydration reactions.
10
11 Nevertheless, photocatalysis usually involves oxidation/reduction reactions induced by
12
13 photogenerated holes and electrons, respectively,^{4, 20} which limits its use in the synthesis of complex
14
15 products from readily available feedstocks. If redox catalytic sites work separately, BAL was finally
16
17 converted to benzoin (BZ) or benzil.^{4, 21} Therefore, rationally assembling oxidation and reduction
18
19 reactions in sequence is the key to produce DOB from BAL. A solution is to develop semiconductors
20
21 of which the properties can be continuously adjusted,²² thereby achieving the cooperation of oxidation
22
23 and reduction reactions.²³⁻²⁴ Ternary ZnIn_2S_4 is such a kind of semiconductor of which the band
24
25 structures can be adjusted either by replacing zinc or indium with other metals or by varying the ratio
26
27 of zinc and indium contents.²⁵ The catalyst was used to catalyze coupling of phenylacetylene and
28
29 benzyl mercaptan,²⁶ dehydrocoupling of benzylamine to imidazole,²⁷ and methylfurans to diesel fuel
30
31 precursors by our group.²⁵ Particularly, ZnIn_2S_4 can catalyze the self-transfer hydrogenolysis of lignin
32
33 β -O-4 models, which involves consecutive dehydrogenation of CH-OH moiety and reductive
34
35 hydrogenolysis of C-OAr bond.²⁸ Therefore, rationally adjusting the band structures of ZnIn_2S_4
36
37 semiconductor has a great potential to produce DOB directly from BAL.
38
39
40
41
42
43
44
45
46
47

48 Herein, by tuning the conduction band (CB) bottom potentials of ZnIn sulfides, we successfully
49
50 synthesized DOB from BAL with coproduction of H_2 by visible light irradiation. This process was
51
52 directed to consecutive dehydrocoupling and dehydration reactions rather than dehydrogenation in the
53
54 second step to yield BZ. The dehydrocoupling of BAL to intermediate hydrobenzoin (HB) was realized
55
56 by one-step oxidation by holes followed by C-C coupling while the dehydration of HB was a redox-
57
58
59
60

neutral process that consumed an electron-hole pair. The major product could be controlled to BZ if ZnIn sulfides with larger CB bottom potential was used.

EXPERIMENTAL SECTION

Materials. $\text{ZnSO}_4 \cdot 7\text{H}_2\text{O}$ (99.5%), $\text{InCl}_3 \cdot 4\text{H}_2\text{O}$ (99.9%), thioacetamide (TAA, 99%), cetyl trimethyl ammonium bromide (CTAB), benzyl alcohol (BAL, 99%), 4-methoxyl acetophenone, $\text{Ru(II)Cl}_2(\text{PPh}_3)_2$, D_2O , 4-methylbenzyl alcohol, 4-methoxylbenzyl alcohol, deoxybenzoin, benzoin, hydrobenzoin, benzil, benzaldehyde, were purchased from Shanghai Aladdin Bio-Chem Technology Co., Ltd. Tetrabutylamine hexafluorophosphate (TBAHFP) was purchased from Alfa Aesar. All the reagents were used as received without further purification.

Preparation of ternary $\text{Zn}_x\text{In}_2\text{S}_{3+x}$ ($x = 0.1, 0.2, 0.4, 0.6$ and 0.8). ZnIn sulfides were prepared with referring to a literature procedure.²⁹ Typically, $\text{ZnSO}_4 \cdot 7\text{H}_2\text{O}$, $\text{InCl}_3 \cdot 4\text{H}_2\text{O}$ and CTAB (260.6 mg) were dissolved in 20 mL of Milli-Q water in a 100-mL beaker and magnetically stirred for 30 min at room temperature. TAA (604.8 mg) was then added into the above solution. After being stirred for another 30 min, the mixture was transferred to a 50-mL stainless Teflon-lined autoclave, tightly sealed and placed in a 160 °C oven for 20 h. The autoclave was then naturally cooled to room temperature. After being washed with absolute ethanol (4×25 mL) and Milli-Q water (2×25 mL), a yellow solid was obtained after being dried in vacuum at 60 °C for 12 h.

Photocatalytic reactions. Photocatalytic reactions were conducted in a home-made LED photoreactor as reported in our previous work.²⁸ Briefly, 0.2 mmol of BAL or 0.1 mmol of HB, 10 mg of catalyst, 1.0 mL of MeCN and magnetic bar were added into the quartz reaction tube, followed by replacing the atmosphere by Ar. The reaction tube was installed on the photoreactor. After irradiation for the

desired time, the products were quantitatively analyzed.

For Hammett plot, the reaction rate constants of BAL with substituents relative to that of BAL were obtained by measuring the conversions of BAL and those with substituents at 0.25 h. For hydrogen kinetic isotope effect (KIE), the conversions of BAL and BAL- d_2 at 0.5 h were used to calculate KIE value.

Radical trapping experiments. The radical intermediates in the photocatalytic dehydrocoupling of BAL were trapped *in situ* by 1,1-diphenylethylene in a scale-up reaction. Briefly, 5 mmol of BAL, 10 mmol of 1,1-diphenylethylene, 100 mg of catalyst, 50 mL of MeCN and magnetic bar were added into the quartz reaction cell, followed by replacing the atmosphere by Ar. After irradiation for 50 h by an 86 W blue LEDs (452 nm, full width at half maximum = 10 nm), the mixture was analyzed by GC-MS. Then the reaction mixture was filtered through a 0.22 μ m Nylon syringe filter to remove the catalyst, followed by purification by column chromatography to separate the adduct of radical intermediate and 1,1-diphenylethylene.

^1H NMR (400 MHz, CDCl_3) δ 7.35 – 7.05 (m, 15 H), 4.41 (dd, J = 8.4, 5.1 Hz, 1 H), 4.09 (dd, J = 9.0, 6.8 Hz, 1 H), 2.52 – 2.28 (m, 2 H), 2.05 (s, 1 H). ^{13}C NMR (101 MHz, CDCl_3) δ 144.81, 144.78, 144.34, 128.71, 128.65, 128.64, 128.16, 127.97, 127.80, 126.44, 126.37, 126.11, 72.38, 47.65, 44.90.

Quantitative analysis of liquid phase products by gas chromatography (GC). BAL, DOB, BZ and HB were quantified by GC equipped with a flame ionization detector (GC-FID, Agilent 7890A). 4-Methoxy acetophenone as the internal standard was added into the reaction systems after photo-irradiation for a desired time, followed by filtration through a 0.22 μ m Nylon syringe filter to remove the catalyst. The reaction system was then analyzed by GC. The following equation was used to

calculate the yield of product.

$$\text{Yield of target product} = \frac{\text{moles of BAL converted to target product}}{\text{moles of BAL added}} \times 100\% \quad (1)$$

Quantitative analysis of H₂. H₂ was quantitatively analyzed by GC equipped with a thermal conductivity detector (GC-TCD, Techcomp 7900) with Ar as the carrier gas. After reaction, He as the internal standard was injected into the reaction system. After 10 minutes, about 15 μL of the gas phase was sampled and analyzed. The produced H₂ can be calculated from the following equation:

$$n(\text{H}_2) = \frac{0.5965 \times I(\text{H}_2) \times \frac{V(\text{He})}{\text{mL}}}{I(\text{He})} \times \frac{101.3}{8.314 \times 298} \text{ mmol} = 0.0244 \times \frac{I(\text{H}_2)}{I(\text{He})} \times \frac{V(\text{He})}{\text{mL}} \text{ mmol} \quad (2)$$

$$\text{Yield of H}_2 = \frac{2 \times \text{moles of BAL converted to H}_2}{\text{moles of BAL added}} \times 100\% \quad (3)$$

Where $n(\text{H}_2)$ is the produced H₂ in the reaction system, mmol; $I(\text{H}_2)$ and $I(\text{He})$ are the TCD response of H₂ and He, respectively. $V(\text{He})$ is the injection volume of He. The yield of H₂ was based on BAL conversion to DOB, so 1 mole of H₂ is produced when 2 moles of BAL is exclusively converted to DOB.

Mott-Schottky measurements. 20 mg of Zn_{0.2}In₂S_{3.2} or Zn_{0.6}In₂S_{3.6} was dispersed in 2 mL of MeCN and vigorously stirred for 16 h followed by ultrasonication for 0.5 h. Thereafter, the suspension was added to a clean fluorine-doped tin oxide (FTO) glass (ultrasonically treated in acetone, ethanol and H₂O for 0.5 h, respectively) followed by spin coating (WS-650MZ-23NPP) at 1500 r min⁻¹ for 30 s. Then the FTO was dried naturally at r.t. for re-spin coating. The above steps were repeated for 15 times for each of the two materials to form a proper film of Zn_{0.2}In₂S_{3.2} or Zn_{0.6}In₂S_{3.6} on the FTO glass. Finally the FTO glass coated with sample was dried in vacuum at 90 °C for 12 h. The electrochemical measurements of the prepared Zn_{0.2}In₂S_{3.2} or Zn_{0.6}In₂S_{3.6} electrode were conducted in 0.1 M TBAHFP/MeCN solution with an electrochemical workstation (PARSTAT MC). A three electrode

system with platinum-plate electrode as the counter electrode and Ag/AgCl electrode as the reference electrode was used for measurements. The frequency, scanning voltage range and test points were 1000 Hz, -0.72 V – 0 V and 80, respectively.

RESULTS AND DISCUSSION

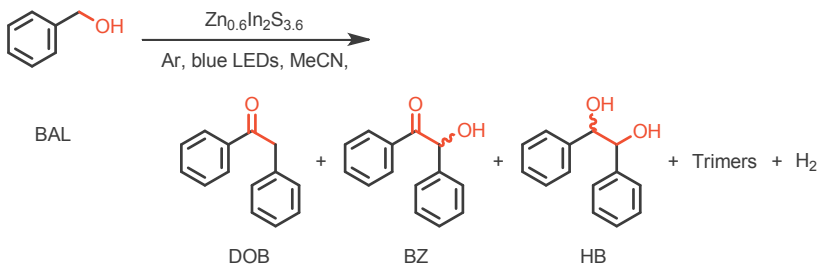
Photocatalyst contrast

Photocatalytic coproduction of H_2 and DOB from BAL was tested with some commonly used semiconductor photocatalysts for comparison. Their BET surface areas and XRD patterns were obtained and shown in Table S1 and Figure S1. In these photocatalysts, BiVO_4 , Bi_2WO_6 and mpg- C_3N_4 (Table 1, entries 1~3) showed low activity in converting BAL to DOB and H_2 . Under the irradiation of UV LEDs ($365 \pm 5\text{ nm}$, 6 W), anatase TiO_2 loaded with Pt by impregnation method converted BAL to benzaldehyde (BA) and H_2 in 73% and 238% yields, respectively (Table 1, entry 4), affording very minor C–C bond coupling products. The missing carbon together with the very high H_2 balance (1.56) may be caused by the over-oxidation of BAL to CO_2 or related acid, which has been reported in other work.³⁰ Irradiation of In_2S_3 with blue LEDs ($450 \pm 5\text{ nm}$, 6 W) for 12 h converted BAL to BA (6% yield) and H_2 (13% yield, Table 1, entry 5). Hydrobenzoin (HB), formed via dehydrocoupling of two BAL molecules, was also generated despite of 2% yield. Reaction over CdS produced HB (31% yield) and H_2 (44% yield) as the major products. Other products were deoxybenzoin (DOB) and trimers (Table 1, entry 6), similar to the reaction results in previous literatures.^{4, 21} By contrast, when the reaction was conducted over $\text{Zn}_{0.2}\text{In}_2\text{S}_{3.2}$ ternary sulfide, BZ and H_2 were the major products (61% and 172% yields, respectively, Table 1, entry 7), the corresponding H_2 balance was determined to be 1.00 (Scheme S2). The yield of DOB was also much higher (30%

1
2
3
4 yield) than that over CdS catalyst. The best result was achieved over $\text{Zn}_{0.6}\text{In}_2\text{S}_{3.6}$ with 64% yield of
5
6
7 DOB produced (Table 1, entry 8). H_2 was produced in 134% yield, lower than that over $\text{Zn}_{0.2}\text{In}_2\text{S}_{3.2}$
8
9 catalyst. This result is consistent with the higher yield of DOB over $\text{Zn}_{0.6}\text{In}_2\text{S}_{3.6}$ catalyst since BAL
10
11 conversion to DOB produces 1 equivalent of H_2 while 2 equivalents when BAL is converted to BZ
12
13 (Scheme S2). The byproducts BZ and trimers were produced in 16% and 13% yields, respectively.
14
15
16
17 Carbon balance and hydrogen balance of this reaction were 95% and 0.99, respectively, the missing
18
19 carbon may go to oligomers due to C–C bond coupling. The reaction did not proceed in the dark (Table
20
21
22 1, entry 9), demonstrating a photocatalytic process.
23
24
25

26 **Table 1. Catalytic performance of some typical semiconductors in photocatalytic coproduction**
27
28 **of H_2 and DOB from BAL.^a**
29

30
31
32
33
34
35
36
37
38
39



The reaction scheme shows BAL (benzyl alcohol) reacting with $\text{Zn}_{0.6}\text{In}_2\text{S}_{3.6}$ under Ar, blue LEDs, and MeCN to produce DOB (1,2-diphenylethan-1-one), BZ (1,2-diphenylethan-1-one-1-ol), HB (1,2-diphenylethan-1,2-diol), trimers, and H_2 .

40
41
42
43
44
45
46
47
48
49
50
51
52
53
54
55
56
57
58
59
60

Entry	Catalyst	Conversion (%)	Yield (%)						H_2 ^c balance
			H_2 ^b	BA	DOB	BZ	HB	Trimer s	
1	BiVO_4	5		4					0
2	Bi_2WO_6	7		3					0
3	mpg- C_3N_4	13		3					0
4 ^d	Pt/P25	99	238	73	1	3	1		1.56
5	In_2S_3	11	13	6			2		0.96
6	CdS	39	44	1	2		31	5	0.94
7	$\text{Zn}_{0.2}\text{In}_2\text{S}_{3.2}$	> 99	172	9	30	61			1.00
8	$\text{Zn}_{0.6}\text{In}_2\text{S}_{3.6}$	> 99	134	2	64	16		13	0.99

9^e Zn_{0.6}In₂S_{3.6} 7 2 0

^a Reaction conditions: 0.2 mmol of BAL, 10 mg of catalyst, 1.0 mL of MeCN, Ar atmosphere, 6 W blue LEDs (455 ± 5 nm), 12 h. ^b The calculation of H₂ yield was based on the conversion of BAL to DOB (stoichiometric ratio of H₂ and DOB is 1:2), so the theoretical yield of H₂ is 100% when DOB is produced in 100% yield. ^c H₂ balance = yield (H₂) / [2×yield (BA) + yield (DOB) + 2×yield (BZ) + yield (HB) + 8/3×yield (trimers)]. ^d 6 W LEDs (365 ± 5 nm). ^e Reaction in the dark. The procedures for the preparation of control catalysts can be found in Supporting Information.

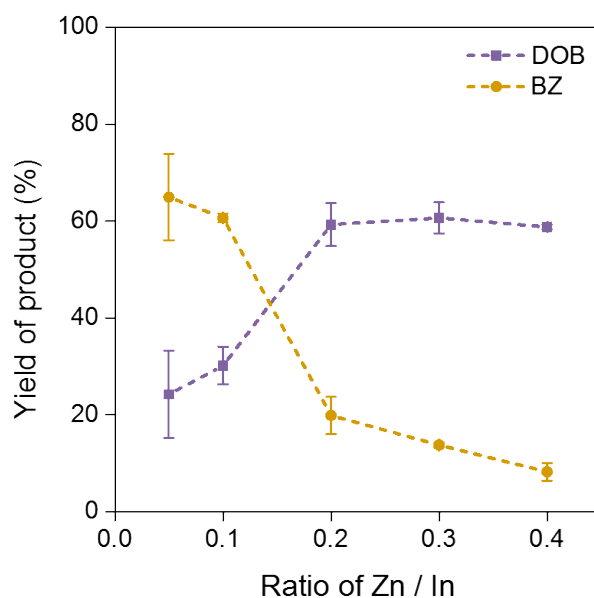


Figure 1. Influence of Zn/In ratio on product yields in photocatalytic dehydrocoupling of BAL to DOB and BZ. Reaction conditions: 0.2 mmol of BAL, 10 mg of catalyst, 1.0 mL of MeCN, Ar atmosphere, 6 W blue LEDs (455 ± 5 nm), 9 h.

Variation of Zn/In ratio of ternary ZnIn sulfides greatly altered selectivity towards DOB and BZ according to Table 1, entries 7 and 8. As a result, a higher Zn/In ratio favors the formation of DOB. The influence of Zn/In ratio was further studied. Zn_xIn₂S_{3+x} with various x were prepared by the same hydrothermal method except varying the relative contents of zinc and indium precursors (Table S1).

According to X-ray diffraction (XRD), field emission scanning electron microscope (FE-SEM) and transmission electron microscope (TEM) results (Figure S2 and S3), the structures of the series of ternary ZnIn sulfides are similar to hexagonal ZnIn_2S_4 ,²⁹ but contains minor $\beta\text{-In}_2\text{S}_3$ phase.³¹ Their band gaps widen from 2.27 to 2.40 eV when x varies from 0.1 to 0.8 (Figure S4). The ternary $\text{Zn}_x\text{In}_{2-x}\text{S}_3$ with $x = 0.1, 0.2, 0.4, 0.6$ and 0.8 were employed for photocatalytic dehydrocoupling of BAL to DOB (Figure 1). When $\text{Zn}_{0.1}\text{In}_{1.9}\text{S}_3$ ($\text{Zn/In} = 0.05$) was used, DOB was produced in 24% yield and the major product was BZ (65% yield). Other products were mainly BA (7% yield), implying predominant dehydrogenation than dehydration over $\text{Zn}_{0.1}\text{In}_{1.9}\text{S}_3$ catalyst. Reaction over $\text{Zn}_{0.2}\text{In}_{1.8}\text{S}_3$ offered similar distributions of products as previously discussed. By contrast, ZnIn sulfide with a higher zinc content ($x \geq 0.4$) produced 59% DOB yield accompanied by the BZ yield decreased to 8%. Therefore, we show that the main product can be switched between DOB and BZ by altering the zinc content of ZnIn sulfide catalysts.

Exploration of reaction path

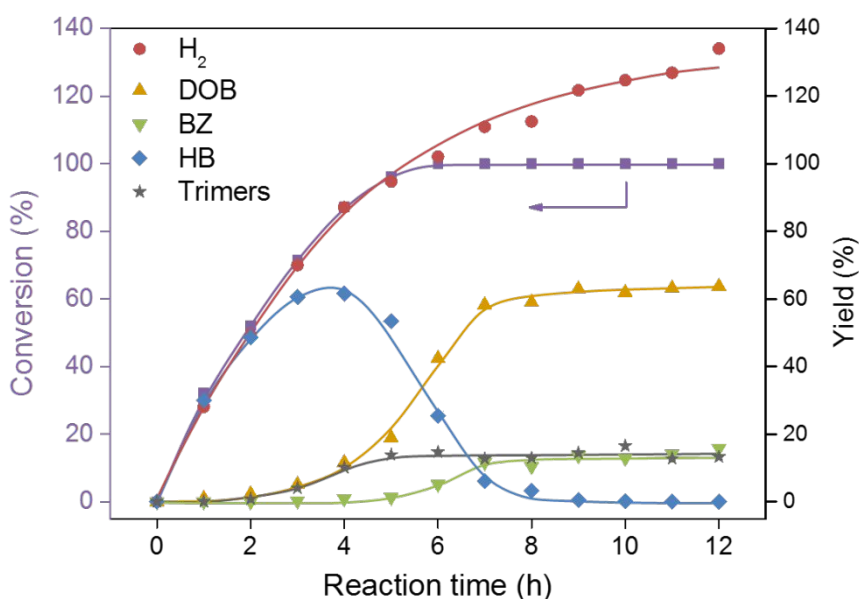
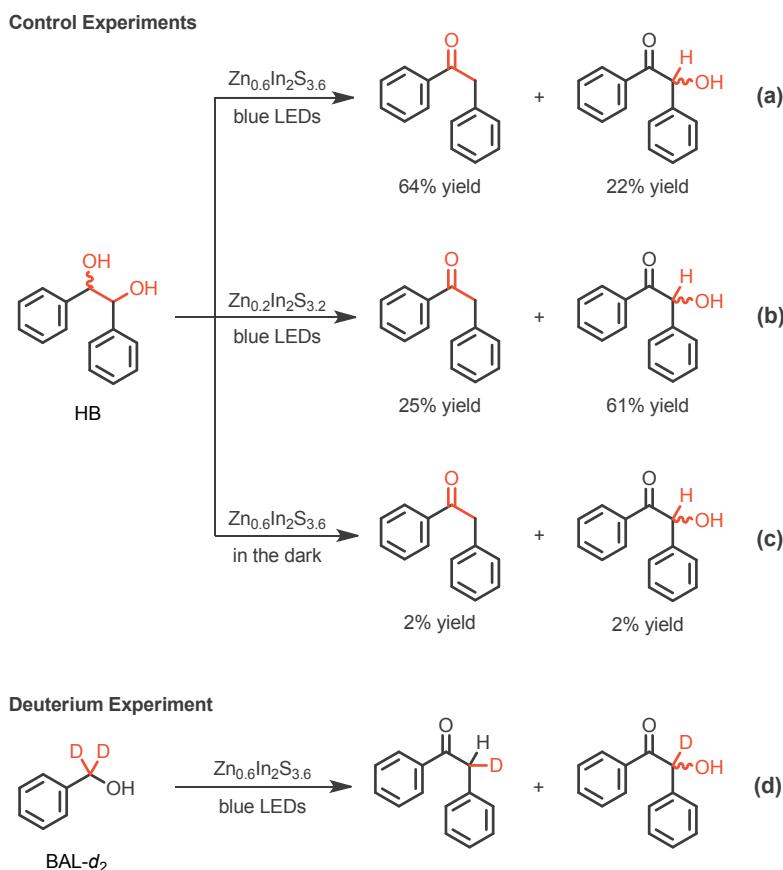


Figure 2. Time profile of photocatalytic dehydrocoupling of BAL over $\text{Zn}_{0.6}\text{In}_{1.4}\text{S}_3$ catalyst. Reaction

1
2
3
4 conditions: 0.2 mmol of BAL, 10 mg of $\text{Zn}_{0.6}\text{In}_2\text{S}_{3.6}$, 1.0 mL of MeCN, Ar atmosphere, 6 W blue LEDs
5
6 (455 \pm 5 nm). All the data points are the average of two separated experiments. Curves drawn on top
7
8 of data are guides to the eye.
9
10

11
12 Targeting DOB, the time profile of photocatalytic dehydrocoupling of BAL over $\text{Zn}_{0.6}\text{In}_2\text{S}_{3.6}$
13 catalyst was studied (Figure 2). After lighting on, BAL was rapidly converted, accompanied by the
14
15 formation of HB and H_2 . HB showed a maximum yield (62% yield) after the LEDs irradiation for 4 h.
16
17 Afterwards, HB diminished and the main product DOB, byproducts BZ and trimers appeared, together
18
19 with the formation of additional H_2 . The time profiles of DOB and BZ show induction periods at the
20
21 same time range, implying that DOB and BZ are produced from HB in consecutive reactions.²¹ BZ
22
23 generation can be rationalized by the second-step dehydrogenation of the hydroxyl group in HB
24
25 (Scheme S3) by photogenerated holes as described in previous work.²¹ DOB is the dehydration product
26
27 of HB, but the mechanism is less known as photocatalytic dehydration is rarely reported.³² After
28
29 reaction for 12 h, the yields of the three liquid phase products all reached constant values with total
30
31 conversion of BAL.
32
33
34
35
36
37
38
39
40
41
42
43
44
45
46
47
48
49
50
51
52
53
54
55
56
57
58
59
60



Scheme 1. Investigation of reaction path. Reaction conditions: 0.2 mmol of BAL, 10 mg of $\text{Zn}_{0.6}\text{In}_2\text{S}_{3.6}$, 1.0 mL of MeCN, Ar atmosphere, 6 W blue LEDs (455 ± 5 nm), 9 h.

HB as the intermediate for the formation of DOB and BZ was confirmed by control experiments. With HB subjected to reaction over $\text{Zn}_{0.6}\text{In}_2\text{S}_{3.6}$ catalyst under the irradiation of blue LEDs (455 nm), DOB and BZ were formed in 64% and 22% yields, respectively, similar to the case of BAL substrate (Scheme 1a). Other byproducts were not detected in GC and might be oligomers due to homo-coupling of two HB after the cleavage of the benzylic C–H bond. Reaction over $\text{Zn}_{0.2}\text{In}_2\text{S}_{3.2}$ catalyst afforded BZ in 61% yield (Scheme 1b). The above results well explain the variation of product yields over the ZnIn sulfides with different Zn/In ratios in Figure 1. When the reaction was conducted over $\text{Zn}_{0.6}\text{In}_2\text{S}_{3.6}$ catalyst in the dark, HB was only slightly converted with very low yields of DOB and BZ (Scheme 1c), implying dehydration of HB to DOB proceeds in a photocatalytic manner.

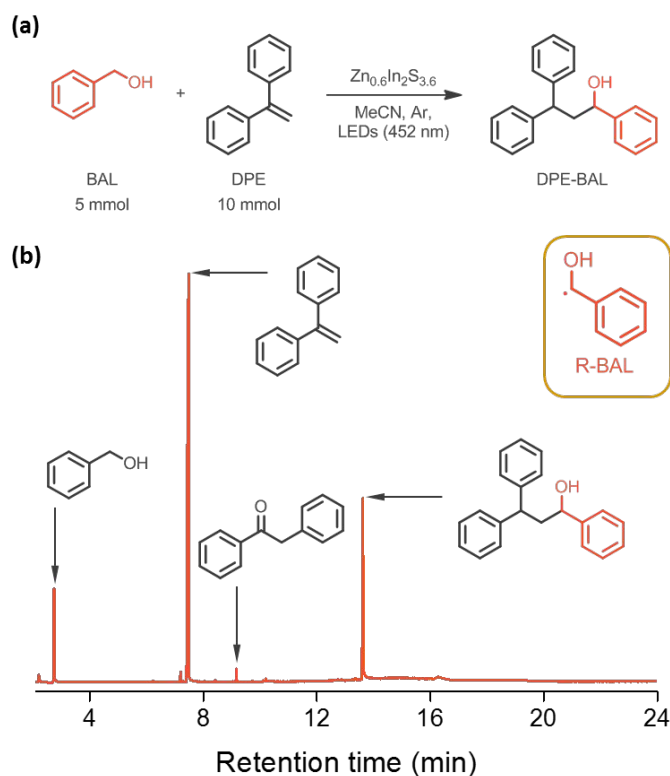


Figure 3. Radical capturing results of photocatalytic dehydrocoupling of BAL to DOB. (a) Reaction scheme of radical capturing by 1,1-diphenylethylene. (b) Gas chromatogram of the reaction mixture. Reaction conditions: 100 mg of $\text{Zn}_{0.6}\text{In}_2\text{S}_{3.6}$, 5 mmol of BAL, 10 mmol of 1,1-diphenylethylene, 50 mL of MeCN, Ar, 86 W LEDs (452 ± 10 nm), 84 h.

The reaction mechanism was studied by isotope label experiment, replacing the benzylic hydrogen atoms by deuterium (Scheme 1d). The involvement of only one deuterium atom in DOB is consistent with the reaction process that dehydrocoupling of BAL forms HB followed by the dehydration and enol-keto tautomerism to DOB. BZ also contains one deuterium atom linked to carbon, consistent with the dehydrocoupling-dehydrogenation mechanism for its formation. Substituents at the para-position of BAL show irregular and marginal influence on the reaction rates (Figure S5), confirming a neutral intermediate (radical) involved in the benzylic C–H bond cleavage.³³⁻³⁴ The slower reaction rate of BAL with –OMe substituent may be ascribed to the larger polarity of –OMe which competes with –

CH₂OH group for adsorption on catalyst surface. The radical in photocatalytic BAL dehydrocoupling was captured by 1,1-diphenylethylene (DPE, Figure 3). The addition of 2 equivalents of DPE nearly inhibit the reaction and only a small amount of DOB was produced (Figure 3a), consistent with a radical mechanism for the photocatalytic BAL dehydrocoupling. Besides, the direct detection of DPE-BAL illustrates that photocatalytic dehydrocoupling of BAL to HB involves direct C–H bond activation by photogenerated holes, forming radical R-BAL (Figure 3b). Of note, the hydrogen kinetic isotope effect (KIE) of photocatalytic dehydrocoupling of BAL was determined to be 1.25 ± 0.04 (Scheme S4a), demonstrating that C–H bond activation is not involved in the rate-limiting step.³⁵ Accompanied by the reactions of photogenerated holes, the generated protons produced from C–H bond cleavage was reduced to H₂ by photogenerated electrons (Scheme S3).

Studies of photocatalytic dehydration mechanism

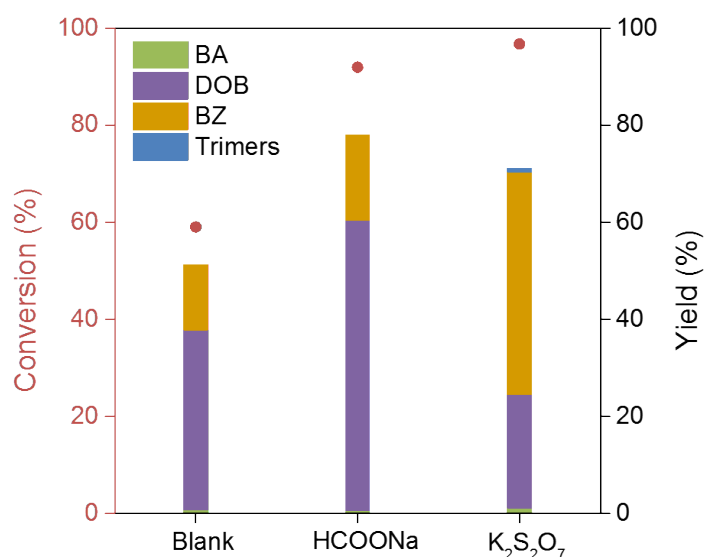


Figure 4. HB (0.1 mmol) conversion in the presence of hole trapping reagent (0.2 mmol of HCOONa) or electron trapping reagent (0.2 mmol of K₂S₂O₈), photo-irradiation for 1 h. Reaction conditions: 0.2 mmol of substrate, 10 mg of Zn_{0.6}In₂S_{3.6}, 1.0 mL of MeCN, Ar atmosphere, 6 W blue LEDs (455 ± 5

nm), 0.25 h.

The dehydration mechanism of intermediate HB to targeted product DOB was studied by radical trapping experiments (Figure 4). Since the valence band (VB) top potentials of the series of ZnIn sulfides lie above the oxidation potential of hydroxyl groups,³⁶⁻³⁷ we considered that HB conversion to either DOB or BZ is initiated by C–H bond activation, in the same way as that of BAL. Addition of hole trapping reagent (HCOONa) into the reaction system accelerated HB conversion to DOB, illustrating that oxidation of HB by photogenerated holes was not involved in the rate-limiting steps, which was proved by the secondary KIE value (1.17 ± 0.12 , Scheme S4b) for the cleavage of the C–H bond of HB. The slight increase of DOB yield from 64% to 71% (prolong the reaction time to 4 h) implies that reduction reactions, more precisely the reductive cleavage of C–OH bond, induced by photogenerated electrons are likely to steer the selectivity of dehydration products. In agreement with this, addition of electron trapping reagent $K_2S_2O_8$, that competes with HB or related intermediates to be reduced, dramatically suppresses the formation of DOB but favors BZ formation.

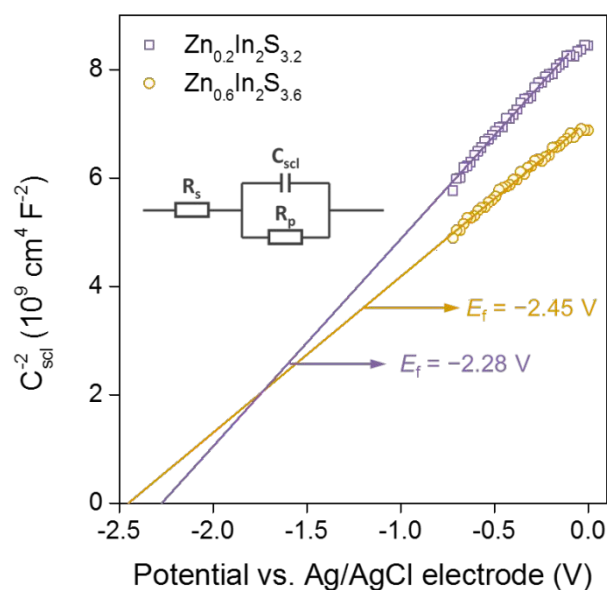


Figure 5. Mott-Schottky plots, the violet and golden yellow lines are tangent lines. The inset shows

the equivalent Randles circuit used to fit the electrochemical impedance data, where R_s is the total series resistance, R_p is the parallel resistance due to the charge transfer, and C_{sc} is the space-charge layer capacitance.

The reaction results of ZnIn sulfides with different Zn/In ratios can be rationalized by their reactivity in the reductive cleavage of C–OH bond. Mott-Schottky method was used to measure the CB bottom potentials of the ZnIn sulfides in MeCN solution, which are located at potentials 0.4 V more negative than the corresponding flat band potentials (E_f , Figure 5).³⁸⁻³⁹ The obtained result of $\text{Zn}_{0.6}\text{In}_2\text{S}_{3.6}$ was -2.85 V, smaller than that of $\text{Zn}_{0.2}\text{In}_2\text{S}_{3.2}$ (-2.68 V), in agreement with previously reported results that a higher Zn/In ratio corresponds to a lower CB bottom potential of the ZnIn sulfide,⁴⁰ which results in the high reduction ability of the catalyst. Therefore, a higher Zn/In ratio favored the reductive cleavage of C–OH bond for the formation of DOB. However, when 1-phenylethanol was subjected to reaction, 2,3-diphenylbutane-2,3-diol was the only product due to C–C bond coupling (Scheme S4c), implying that the catalysts cannot directly reduce the C–OH bond of HB. Therefore, the ZnIn sulfides were likely to reductively cleave the C–OH bond of radical **R_{1b}** (Figure 6) that was generated from HB through C–H bond cleavage. Although CB bottom potential is crucial for the reductive cleavage of C–OH bond, a relatively large light intensity is also important for the photocatalytic dehydration of HB to DOB since solar light cannot afford DOB as the main product (Scheme S5).

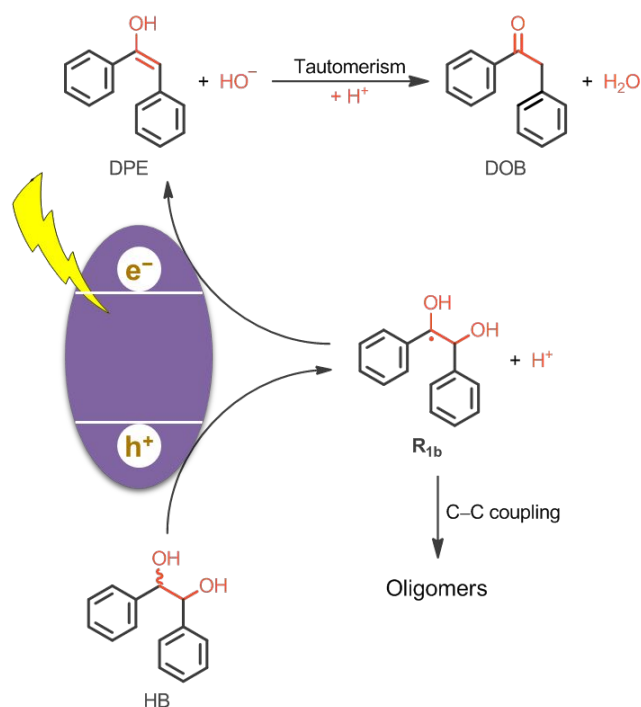


Figure 6. Proposed reaction mechanism of photocatalytic dehydration of intermediate HB to DOB.

The proposed reaction mechanism of HB dehydration to DOB was shown in Figure 6. Photogenerated holes oxidize the C-H bond of HB, delivering radical R_{1b} (Figure 6) that transfers to CB and is reduced to 1,2-diphenylethan-1,2-diol (DPE) by photogenerated electrons. Tautomerism of DPE finally forms DOB. Besides, DOB production from HB involves hole-oxidation and electron-reduction reactions where kinetic factors also counts, thus, the reported method of varying CB bottom potential of ZnIn sulfide only improved DOB yield from 24% to 64%.

Scale-up photocatalytic preparation of DOB derivatives

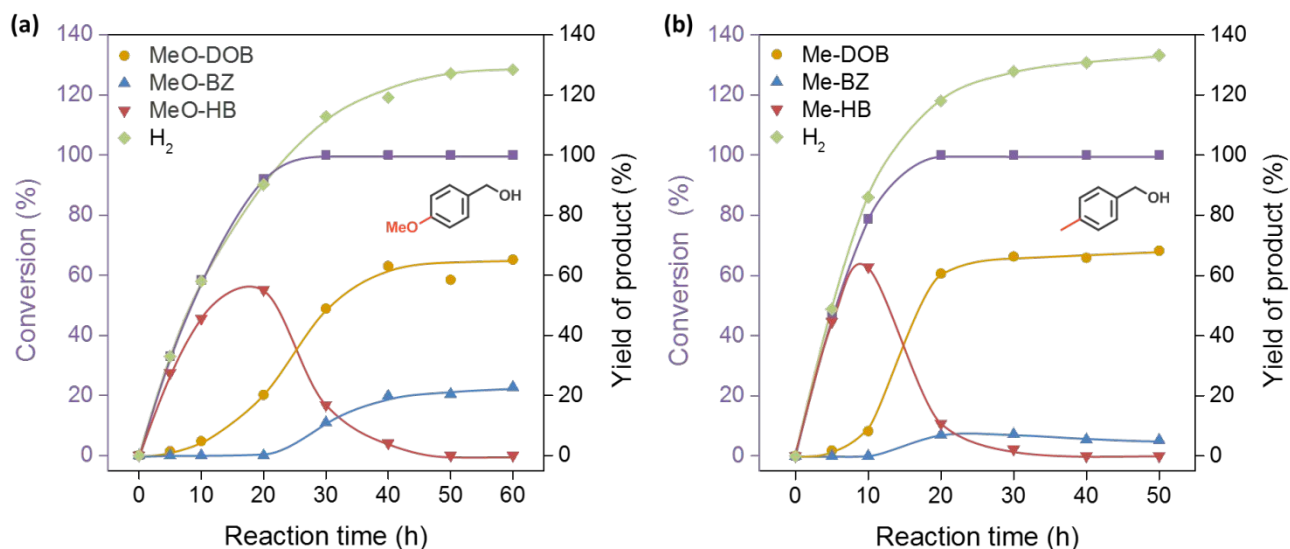


Figure 7. Scale-up reactions of photocatalytic coproduction of substituted DOB and H₂. *p*-Methoxy BAL (a) and *p*-methyl BAL (b) as substrates. Reaction conditions: 10 mmol of substrate, 250 mg of Zn_{0.6}In₂S_{3.6}, 50 mL of MeCN, Ar atmosphere, 86 W blue LEDs (452 ± 10 nm). Inserts show the substrates. The yields of products were quantified by GC. Curves drawn on top of data are guides to the eyes.

The tandem dehydrocoupling-dehydration method was used to synthesize DOB derivatives in scale-up reactions (10 mmol of substrate). Methoxyl and methyl groups were chosen due to the abundance of them in pharmaceuticals. Besides, benzylic methyl group is very active in many photocatalytic systems,^{2, 25} thus, the co-presence of benzylic methyl group can be used to evaluate the selectivity of the catalyst. Figure 7 shows the time profiles in converting *p*-methoxy BAL and *p*-methyl BAL to their corresponding DOB. The product distributions were similar to that of BAL with dominant production of DOB with substituents. Consistent with photocatalytic BAL to DOB, vicinal diols were the intermediates, further confirming the previously proposed reaction mechanism. Particularly, the formed H₂ was 147 mL in the case of *p*-methoxy BAL, higher than that of *p*-methyl BAL (134 mL of

H₂), in agreement with the lower yield of substituted DOB for p-methoxy BAL. The isolated yields of 1,2-bis(4-methoxyphenyl)ethanone and 1,2-di-*p*-tolylethanone were 58% and 65%, respectively. The simultaneous production of H₂ and substituted DOB in gram scale demonstrates the tandem dehydrocoupling-dehydration method in the transformation of readily available feedstocks to value-added products including clean energy vectors and chemicals.

CONCLUSIONS

In summary, we achieved the visible-light photocatalytic production of H₂ from BAL with simultaneously production of DOB, which improved the value of feedstocks. The dehydrocoupling of BAL to HB was the first step involved in the transformation and achieved by selective cleavage of the benzylic C–H bond by photogenerated holes. Subsequent dehydration of HB was the key to the desired product DOB, which was a redox neutral process that consumed an electron-hole pair. Increasing the Zn/In ratio decreased the CB bottom potentials of the ZnIn sulfides, thus facilitating the reduction of hydroxyl groups and directing the major product to DOB under the irradiation of the blue LEDs. Therefore, the main product can be varied between DOB and BZ by altering Zn/In ratio of the ZnIn sulfides. This work puts forward a way to produce renewable H₂ from readily available feedstocks that are simultaneously converted to very valuable products by tandem redox photoreactions.

AUTHOR INFORMATION

Corresponding Author

* F.W. E-mail: wangfeng@dicp.ac.cn

Notes

There are no conflicts to declare.

ASSOCIATED CONTENT

Supporting Information. Catalyst characterization, including XRD, TEM images and some catalytic results. This material is available free of charge via the Internet at <http://pubs.acs.org>.

ACKNOWLEDGMENT

We acknowledge financial support from the National Natural Science Foundation of China (21721004, 21690084, 21690080), the Strategic Priority Research Program of Chinese Academy of Sciences (XDB17020300, XDB17000000). Computing resource from the National Supercomputing Center in Tianjin, China is gratefully acknowledged.

REFERENCES

1. Cherevatskaya, M.; Neumann, M.; Fuedner, S.; Harlander, C.; Kuemmel, S.; Dankesreiter, S.; Pfitzner, A.; Zeitler, K.; Koenig, B. Visible-Light-Promoted Stereoselective Alkylation by Combining Heterogeneous Photocatalysis with Organocatalysis. *Angew. Chem. Int. Ed.* **2012**, *51*, 4062–4066.
2. Liu, Y.; Chen, L.; Yuan, Q.; He, J.; Au, C. T.; Yin, S. F. A Green and Efficient Photocatalytic Route for the Highly-Selective Oxidation of Saturated Alpha-Carbon C-H Bonds in Aromatic Alkanes over Flower-Like Bi₂WO₆. *Chem. Commun.* **2016**, *52*, 1274–1277.
3. Ghosh, I.; Khamrai, J.; Savateev, A.; Shlapakov, N.; Antonietti, M.; König, B. Organic Semiconductor Photocatalyst Can Bifunctionalize Arenes and Heteroarenes. *Science* **2019**, *365*, 360–366.
4. Chai, Z.; Zeng, T.-T.; Li, Q.; Lu, L.-Q.; Xiao, W.-J.; Xu, D. Efficient Visible Light-Driven Splitting of Alcohols into Hydrogen and Corresponding Carbonyl Compounds over a Ni-Modified

CdS Photocatalyst. *J. Am. Chem. Soc.* **2016**, *138*, 10128–10131.

5. Lin, L.; Zhou, W.; Gao, R.; Yao, S.; Zhang, X.; Xu, W.; Zheng, S.; Jiang, Z.; Yu, Q.; Li, Y. W.; Shi, C.; Wen, X. D.; Ma, D. Low-Temperature Hydrogen Production from Water and Methanol Using Pt/ α -MoC Catalysts. *Nature* **2017**, *544*, 80–83.
6. Chen, B.; Wu, L. Z.; Tung, C. H. Photocatalytic Activation of Less Reactive Bonds and Their Functionalization via Hydrogen-Evolution Cross-Couplings. *Acc. Chem. Res.* **2018**, *51*, 2512–2523.
7. Liu, M.; Wang, Y.; Kong, X.; Rashid, R. T.; Chu, S.; Li, C.-C.; Hearne, Z.; Guo, H.; Mi, Z.; Li, C.-J. Direct Catalytic Methanol-to-Ethanol Photo-Conversion via Methyl Carbene. *Chem* **2019**, *5*, 858–867.
8. Xie, S.; Shen, Z.; Deng, J.; Guo, P.; Zhang, Q.; Zhang, H.; Ma, C.; Jiang, Z.; Cheng, J.; Deng, D.; Wang, Y. Visible Light-Driven C-H Activation and C-C Coupling of Methanol into Ethylene Glycol. *Nat. Commun.* **2018**, *9*, 1181.
9. Meng, L.; Chen, Z.; Ma, Z.; He, S.; Hou, Y.; Li, H.-H.; Yuan, R.; Huang, X.-H.; Wang, X.; Wang, X.; Long, J. Gold Plasmon-Induced Photocatalytic Dehydrogenative Coupling of Methane to Ethane on Polar Oxide Surfaces. *Energy Environ. Sci.* **2018**, *11*, 294–298.
10. Li, L.; Fan, S.; Mu, X.; Mi, Z.; Li, C. J. Photoinduced Conversion of Methane into Benzene over GaN Nanowires. *J. Am. Chem. Soc.* **2014**, *136*, 7793–7796.
11. Shih, C. F.; Zhang, T.; Li, J.; Bai, C. Powering the Future with Liquid Sunshine. *Joule* **2018**, *2*, 1925–1949.
12. Zhang, Y.-M.; Li, M.; Li, W.; Huang, Z.; Zhu, S.; Yang, B.; Wang, X.-C.; Zhang, S. X.-A. A New Class of “Electro-Acid/Base”-Induced Reversible Methyl Ketone Colour Switches. *J. Mater. Chem. C* **2013**, *1*, 5309–5314.

13. Allen, C. F. H.; Barker, W. E. Desoxybenzoin. *Org. Syn.* **1932**, *12*, 16.
14. Chen, X.; Chen, Z.; So, C. M. Exploration of Aryl Phosphates in Palladium-Catalyzed Mono-
Alpha-Arylation of Aryl and Heteroaryl Ketones. *J. Org. Chem.* **2019**, *84*, 6337–6346.
15. Miao, T.; Wang, G. W. Synthesis of Ketones by Palladium-Catalysed Desulfitative Reaction of
Arylsulfinic Acids with Nitriles. *Chem. Commun.* **2011**, *47*, 9501–9503.
16. Ding, Y.; Zhang, W.; Li, H.; Meng, Y.; Zhang, T.; Chen, Q.-Y.; Zhu, C. Metal-Free Synthesis of
Ketones by Visible-Light Induced Aerobic Oxidative Radical Addition of Aryl Hydrazines to Alkenes.
Green Chem. **2017**, *19*, 2941–2944.
17. Han, G.; Jin, Y. H.; Burgess, R. A.; Dickenson, N. E.; Cao, X. M.; Sun, Y. Visible-Light-Driven
Valorization of Biomass Intermediates Integrated with H₂ Production Catalyzed by Ultrathin Ni/CdS
Nanosheets. *J. Am. Chem. Soc.* **2017**, *139*, 15584–15587.
18. Zheng, Y. W.; Chen, B.; Ye, P.; Feng, K.; Wang, W.; Meng, Q. Y.; Wu, L. Z.; Tung, C. H.
Photocatalytic Hydrogen-Evolution Cross-Couplings: Benzene C–H Amination and Hydroxylation. *J.*
Am. Chem. Soc. **2016**, *138*, 10080–10083.
19. Gunanathan, C.; Milstein, D. Applications of Acceptorless Dehydrogenation and Related
Transformations in Chemical Synthesis. *Science* **2013**, *341*, 1229712.
20. Li, L.; Wang, Y.; Vanka, S.; Mu, X.; Mi, Z.; Li, C. J. Nitrogen Photofixation over III-Nitride
Nanowires Assisted by Ruthenium Clusters of Low Atomicity. *Angew. Chem. Int. Ed.* **2017**, *56*, 8701–
8705.
21. Mitkina, T.; Stanglmair, C.; Setzer, W.; Gruber, M.; Kisch, H.; Koenig, B. Visible Light Mediated
Homo- and Heterocoupling of Benzyl Alcohols and Benzyl Amines on Polycrystalline Cadmium
Sulfide. *Org. Biomol. Chem.* **2012**, *10*, 3556–3561.

22. Wang, Y.; Silveri, F.; Bayazit, M. K.; Ruan, Q.; Li, Y.; Xie, J.; Catlow, C. R. A.; Tang, J. Bandgap Engineering of Organic Semiconductors for Highly Efficient Photocatalytic Water Splitting. *Adv. Energy. Mater.* **2018**, *8*, 1801084.
23. Zhang, Z.; Edme, K.; Lian, S.; Weiss, E. A. Enhancing the Rate of Quantum-Dot-Photocatalyzed Carbon-Carbon Coupling by Tuning the Composition of the Dot's Ligand Shell. *J. Am. Chem. Soc.* **2017**, *139*, 4246–4249.
24. Janssens, W.; Makshina, E. V.; Vanelderen, P.; De Clippel, F.; Houthoofd, K.; Kerkhofs, S.; Martens, J. A.; Jacobs, P. A.; Sels, B. F. Ternary Ag/MgO-SiO₂ Catalysts for the Conversion of Ethanol into Butadiene. *ChemSusChem* **2015**, *8*, 994–1008.
25. Luo, N.; Montini, T.; Zhang, J.; Fornasiero, P.; Fonda, E.; Hou, T.; Nie, W.; Lu, J.; Liu, J.; Heggen, M.; Lin, L.; Ma, C.; Wang, M.; Fan, F.; Jin, S.; Wang, F. Visible-Light-Driven Coproduction of Diesel Precursors and Hydrogen from Lignocellulose-Derived Methylfurans. *Nat. Energy* **2019**, *4*, 575–584.
26. Li, Y.; Cai, J.; Hao, M.; Li, Z. Visible Light Initiated Hydrothiolation of Alkenes and Alkynes over ZnIn₂S₄. *Green Chem.* **2019**, *21*, 2345–2351.
27. Wang, M.; Li, L.; Lu, J.; Luo, N.; Zhang, X.; Wang, F. Photocatalytic Coupling of Amines to Imidazoles Using a Mo–ZnIn₂S₄ Catalyst. *Green Chem.* **2017**, *19*, 5172–5177.
28. Luo, N.; Wang, M.; Li, H.; Zhang, J.; Hou, T.; Chen, H.; Zhang, X.; Lu, J.; Wang, F. Visible-Light-Driven Self-Hydrogen Transfer Hydrogenolysis of Lignin Models and Extracts into Phenolic Products. *ACS Catal.* **2017**, *7*, 4571–4580.
29. Gou, X.; Cheng, F.; Shi, Y.; Zhang, L.; Peng, S.; Chen, J.; Shen, P. Shape-Controlled Synthesis of Ternary Chalcogenide ZnIn₂S₄ and CuIn(S,Se)₂ Nano-/Microstructures via Facile Solution Route. *J. Am. Chem. Soc.* **2006**, *128*, 7222–7229.

30. Tsukamoto, D.; Ikeda, M.; Shiraishi, Y.; Hara, T.; Ichikuni, N.; Tanaka, S.; Hirai, T. Selective Photocatalytic Oxidation of Alcohols to Aldehydes in Water by TiO₂ Partially Coated with WO₃. *Chem. Eur. J.* **2011**, *17*, 9816–9824.
31. Horani, F.; Lifshitz, E. Unraveling the Growth Mechanism Forming Stable γ -In₂S₃ and β -In₂S₃ Colloidal Nanoplatelets. *Chem. Mater.* **2019**, *31*, 1784–1793.
32. Bai, H.; Su, N.; Li, W.; Zhang, X.; Yan, Y.; Li, P.; Ouyang, S.; Ye, J.; Xi, G. W₁₈O₄₉ Nanowire Networks for Catalyzed Dehydration of Isopropyl Alcohol to Propylene under Visible Light. *J. Mater. Chem. A* **2013**, *1*, 6125–6129.
33. Hansch, C.; Leo, A.; Taft, R. W. A Survey of Hammett Substituent Constants and Resonance and Field Parameters. *Chem. Rev.* **1991**, *91*, 165–195.
34. Shimoyama, Y.; Ishizuka, T.; Kotani, H.; Kojima, T. Catalytic Oxidative Cracking of Benzene Rings in Water. *ACS Catal.* **2018**, *9*, 671–678.
35. Hou, T.; Luo, N.; Li, H.; Heggen, M.; Lu, J.; Wang, Y.; Wang, F. Yin and Yang Dual Characters of CuO_x Clusters for C–C Bond Oxidation Driven by Visible Light. *ACS Catal.* **2017**, *7*, 3850–3859.
36. Li, X.; Yu, J.; Jaroniec, M. Hierarchical Photocatalysts. *Chem. Soc. Rev.* **2016**, *45*, 2603–2636.
37. Wu, X.; Fan, X.; Xie, S.; Lin, J.; Cheng, J.; Zhang, Q.; Chen, L.; Wang, Y. Solar Energy-Driven Lignin-First Approach to Full Utilization of Lignocellulosic Biomass under Mild Conditions. *Nature Catalysis* **2018**, *1*, 772–780.
38. Matsumoto, Y.; Omae, M.; Watanabe, I.; Sato, E.-i. Photoelectrochemical Properties of the Zn-Ti-Fe Spinel Oxides. *J. Electrochem. Soc.: Electrochem. Sic. Technol.* **1986**, *133*, 711–716.
39. Matsumoto, Y. Energy Positions of Oxide Semiconductors and Photocatalysis with Iron Complex Oxides. *J. Solid State Chem.* **1996**, *126*, 227–234.

- 1
2
3
4 40. Shen, S.; Zhao, L.; Guo, L. $\text{Zn}_m\text{In}_2\text{S}_{3+m}$ ($m=1-5$, Integer): A New Series of Visible-Light-Driven
5
6 Photocatalysts for Splitting Water to Hydrogen. *Int. J. Hydrogen Energy* **2010**, *35*, 10148–10154.
7
8
9
10
11
12
13
14
15
16
17
18
19
20
21
22
23
24
25
26
27
28
29
30
31
32
33
34
35
36
37
38
39
40
41
42
43
44
45
46
47
48
49
50
51
52
53
54
55
56
57
58
59
60

Graphical abstract

